A 3D QSAR Study on a Set of Dopamine D_4 Receptor Antagonists

Jonas Boström,*,†,§ Markus Böhm,‡,# Klaus Gundertofte,† and Gerhard Klebe‡

H. Lundbeck A/S, Ottiliavej 9, DK-2500 Copenhagen-Valby, Denmark, and Department of Pharmaceutical Chemistry, University of Marburg, Marbacher Weg 6, D-35032 Marburg, Germany

Received January 13, 2003

The molecular alignments obtained from a previously reported pharmacophore model have been employed in a three-dimensional quantitative structure−activity relationship (3D QSAR) study, to obtain a more detailed insight into the structure−activity relationships for D_2 and D_4 receptor antagonists. The frequently applied CoMFA method and the related CoMSIA method were used. Statistically significant models have been derived with these two methods, based on a set of 32 structurally diverse D_2 and D_4 receptor antagonists. The CoMSIA and the CoMFA methods produced equally good models expressed in terms of q^2 values. The predictive power of the derived models were demonstrated to be high. Graphical interpretation of the results, provided by the CoMSIA method, brings to light important structural features of the compounds related to either low- or high-affinity D_2 or D_4 antagonism. The results of the 3D QSAR studies indicate that bulky *N*-substituents decrease D_2 binding, whereas D_4 binding is enhanced. Electrostatically favorable and unfavorable regions exclusive to D_2 receptor binding were identified. Likewise, certain hydrogen-bond acceptors can be used to lower D_2 affinity. These observations may be exploited for the design of novel dopamine D_4 selective antagonists.

INTRODUCTION

The predominant theory among pharmacologists is that neurochemical imbalances in the brain are responsible for schizophrenia. The therapeutic effect of all existing antipsychotics is believed to result from antagonism of dopamine receptors, leading to a dopamine hypothesis of schizophrenia.[1] The crux of the dopamine hypothesis is that the symptoms of schizophrenia are due to dopaminergic hyperactivity in the brain.

Recently, the dopamine D_4 receptor has received great attention as a potential target for novel antipsychotics, leading to a dopamine D_4 hypothesis of schizophrenia.[2−5] The dopamine D_4 hypothesis may be seen as a refinement of the dopamine hypothesis. The classical antipsychotics frequently cause a variety of movement disorders, termed extrapyramidal side effects (EPS). It has been proposed that these side effects are due to blockade of dopamine D_2 receptors in the striatum.[6] Distribution studies indicate that the D_4 subtype is more abundant in the limbic and the cortical brain areas than in the striatum.[7] The antipsychotic clozapine (**1**) shows a highly favorable clinical profile on account of its low EPS liability. Clozapine has been reported to display higher affinity for the D_4 subtype of dopamine receptors than for the D_2 subtype.[2] It is hypothesized that selective D_4 receptor antagonists may be effective antipsychotics without the extrapyramidal side effects observed for the classical antipsychotics (those which generally display high affinity for the D_2 receptor). While clozapine has been found to be very effective, a life threatening decrease in the number of white blood cells (agranulocytosis) has been observed in approximately 1% of the patients.[8] Because of the significant risk of (drug-induced) agranulocytosis schizophrenic patients using clozapine need routine blood monitoring. The drug is therefore of limited therapeutical use. Consequently, recent years have seen a large activity in the development of novel D_4 selective antagonists.[3−5]

We have recently reported a pharmacophore model for several structurally diverse dopamine D_4 antagonists.[9] The molecular alignments obtained from this pharmacophore model have been applied here in a 3D QSAR study, using the CoMFA[10] and the CoMSIA[11] methodologies. Lanig and co-workers recently reported a reasonably successful CoMFA study on a set of structurally homologous dopamine D_4 antagonists,[12] in contrast to our interest in generating a model for structurally diverse D_2 and D_4 receptor antagonists.

The aim of this study is to develop predictive 3D QSAR models to rationalize receptor−ligand interactions of D_4 receptor antagonists and in particular to pinpoint which structural features are responsible for selective D_4 antagonism vs D_2 receptor binding. The CoMFA and CoMSIA methods are compared with each other to see if either gives significantly better statistical results. The CoMSIA method allows for more intuitive graphical interpretation and was the tool of choice for rationalizing the observed high or low affinities of the D_2 and D_4 receptor antagonists of the present study. The ultimate goal is the design of selective, high-affinity D_4 receptor antagonists with a superior clinical profile for the treatment of schizophrenia, with the assistance of the 3D QSAR models developed herein.

* Corresponding author phone: +46 31 706 52 51; fax: +46 31 776 37 10; e-mail: jonas.bostrom@astrazeneca.com.
† H. Lundbeck A/S.
‡ University of Marburg.
§ Present address: AstraZeneca R&D Mölndal, S-431 83 Mölndal, Sweden.
# Present address: Pfizer Inc., Groton, CT 06340.

10.1021/ci034004+ CCC: $25.00
Published on Web 05/02/2003

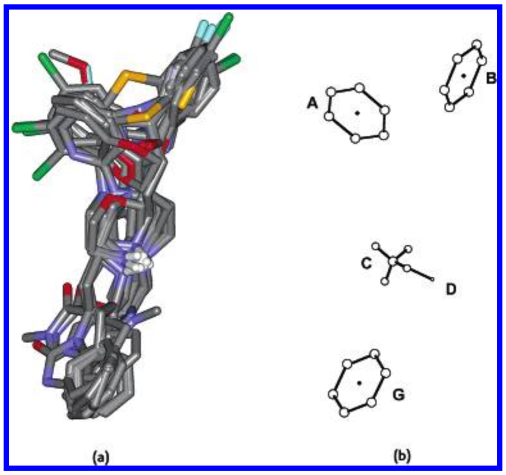

Figure 1. (a) Molecular alignment used in the present study, obtained from the dopamine D_4 pharmacophore model. (b) The basic D_4 pharmacophore model includes five pharmacophore elements, three elements (**A**, **B**, and **G**) corresponding to the aromatic rings, an ammonium nitrogen (**C**), and a site-point in the N−H direction (**D**). The site-point **D** represents a hydrogen-bond acceptor within the receptor.

METHODS

The Dopamine D_4 Pharmacophore Model. We have recently reported a pharmacophore model for dopamine D_4 antagonists.[9] By using exhaustive conformational analyses and least-squares molecular superimposition studies, a large number of structurally diverse high-affinity D_4 antagonists was successfully accommodated in the D_4 pharmacophore model. It was concluded that the bioactive conformations of antagonists at the D_2 and D_4 receptor subtypes are virtually identical. The molecular alignments obtained from this pharmacophore model are employed in the present study (Figure 1a).

The basic dopamine D_4 pharmacophore model includes five pharmacophore elements, three elements (**A**, **B**, and **G**) corresponding to aromatic rings, an ammonium nitrogen (**C**), and a site-point in the N−H direction (**D**) (Figure 1b). The site point **D** represents a hydrogen-bond acceptor site within the receptor cavity, which is assumed to interact with the ammonium nitrogen in the ligand when binding. The dopamine D_4 ligands can adopt three different binding modes with respect to the aromatic pharmacophore elements **A**, **B**, and **G**.[9]

Selection of the Compounds. A total of 32 structurally diverse D_4 and D_2 receptor antagonists were selected for the training set (Figure 2) based on a number of criteria as follows. A correct molecular alignment is of the utmost importance for creating useful and predictive models of biological activity; accordingly all 32 molecules comply with the criterion of being able to adopt the geometry of the previously reported pharmacophore model for dopamine D_4 receptor antagonists.[9] To obtain an even distribution, the ligands of the training set were selected such that approximately one-third represents each of the three possible binding modes.

As a rule of thumb, a spread in affinity of at least three logarithmic units is considered necessary for developing a statistically significant 3D QSAR model. The D_2 receptor affinities spread over a range of nearly five logarithmic units, whereas the D_4 ligands cover three logarithmic units. The

Table 1. Experimental and Calculated Binding Constants, Given as pK_i Values, for the Dopamine D_2 and D_4 Training Set Derived with CoMSIA and CoMFA

	pK_i						
	D_2			D_4			
		calc			calc		
no.	exp	CoMSIA	CoMFA	exp	CoMSIA	CoMFA	ref[a]
1	6.66	7.14	7.23	7.68	7.88	7.84	3
2	8.60	8.47	8.79	7.46	8.15	8.15	2
3	8.89	7.95	7.74	8.19	7.82	7.71	13, 14
4	7.37	8.22	8.13	7.10	8.06	7.90	13, 14
5	6.28	6.89	7.30	7.68	7.80	7.85	15
6	7.33	7.10	7.30	7.80	7.86	7.86	3
7	7.68	7.07	7.28	8.31	7.77	7.84	3
8	8.43	8.15	7.72	7.89	7.84	7.83	13, 16
9	8.18	8.20	8.04	7.96	7.84	7.69	13, 14
10	8.92	8.30	8.41	8.41	7.85	7.80	13, 17
11	6.82	7.18	7.30	7.64	7.94	7.94	3
12	7.29	7.56	7.15	9.00	8.71	8.65	13, 18
13	6.10	6.55	6.98	8.66	8.29	8.74	19
14	8.55	8.42	7.99	8.48	9.25	8.97	13, 20
15	6.04	6.70	6.28	8.44	8.12	8.13	21
16	6.80	6.12	6.56	8.52	8.42	8.77	19
17	6.60	6.04	6.14	8.28	7.95	8.22	22
18	5.66	5.75	6.57	8.07	7.97	8.32	22
19	5.84	5.61	6.33	8.22	8.25	8.26	22
20	7.83	7.28	7.00	8.96	8.71	8.65	13, 18
21	7.10	7.83	7.30	9.05	8.71	8.64	13, 18
22	5.84	6.80	6.75	7.59	8.48	8.49	21
23	10.30	9.74	9.28	10.30	9.26	8.92	2
24	8.89	8.17	8.74	8.75	9.17	9.12	13, 16
25	7.22	6.60	6.38	8.00	7.69	7.80	23
26	6.07	6.45	5.94	7.66	7.66	7.66	23
27	6.05	6.18	6.01	7.64	7.68	7.71	23
28	5.89	6.29	6.04	7.28	7.73	7.79	23
29	6.40	8.09	8.14	8.25	8.56	8.69	24
30	9.82	9.61	9.74	9.38	9.78	9.48	25
31	6.28	6.79	6.07	8.26	7.56	7.53	23
32	7.19	6.35	5.82	7.72	7.72	7.70	23

[a] Where two references are given, this denotes a compound tested at H. Lundbeck A/S (first reference) and listed structurally elsewhere (second reference).

correlation coefficients between the D_2 and D_4 receptor affinities for the compounds in the training set was calculated to be 0.52. The binding affinities for the training set are given in Table 1. The biological data were collected from several different sources (Table 1). Traditionally, external test sets are used to check the predictive power of models derived from training sets; the nine ligands depicted in Figure 3 were chosen for this purpose. The binding affinities for the test sets are given in Tables 2 and 3.

Computational Procedures. All calculations were performed using SYBYL version 6.5[29] running on a Silicon Graphics Octane (R10000). The structural alignment was obtained by fitting the molecules on to the pharmacophore model (Figure 1). The least-squares rigid body superimposition procedure implemented in SYBYL was used. The *N*-protonated forms of the molecules, which are the prevalent species at physiological pH, were used in the calculations. Partial charges were calculated using the AM1 method as implemented in the MOPAC package.[30,31] The grid spacings were 1 Å in all cases. A common grid box was prepared manually to allow for a straightforward comparison between CoMFA and CoMSIA results. The CoMFA calculations were performed with the SYBYL standard parameters (TRIPOS standard field, dielectric constant $1/r$, cutoff 30 kcal/mol)

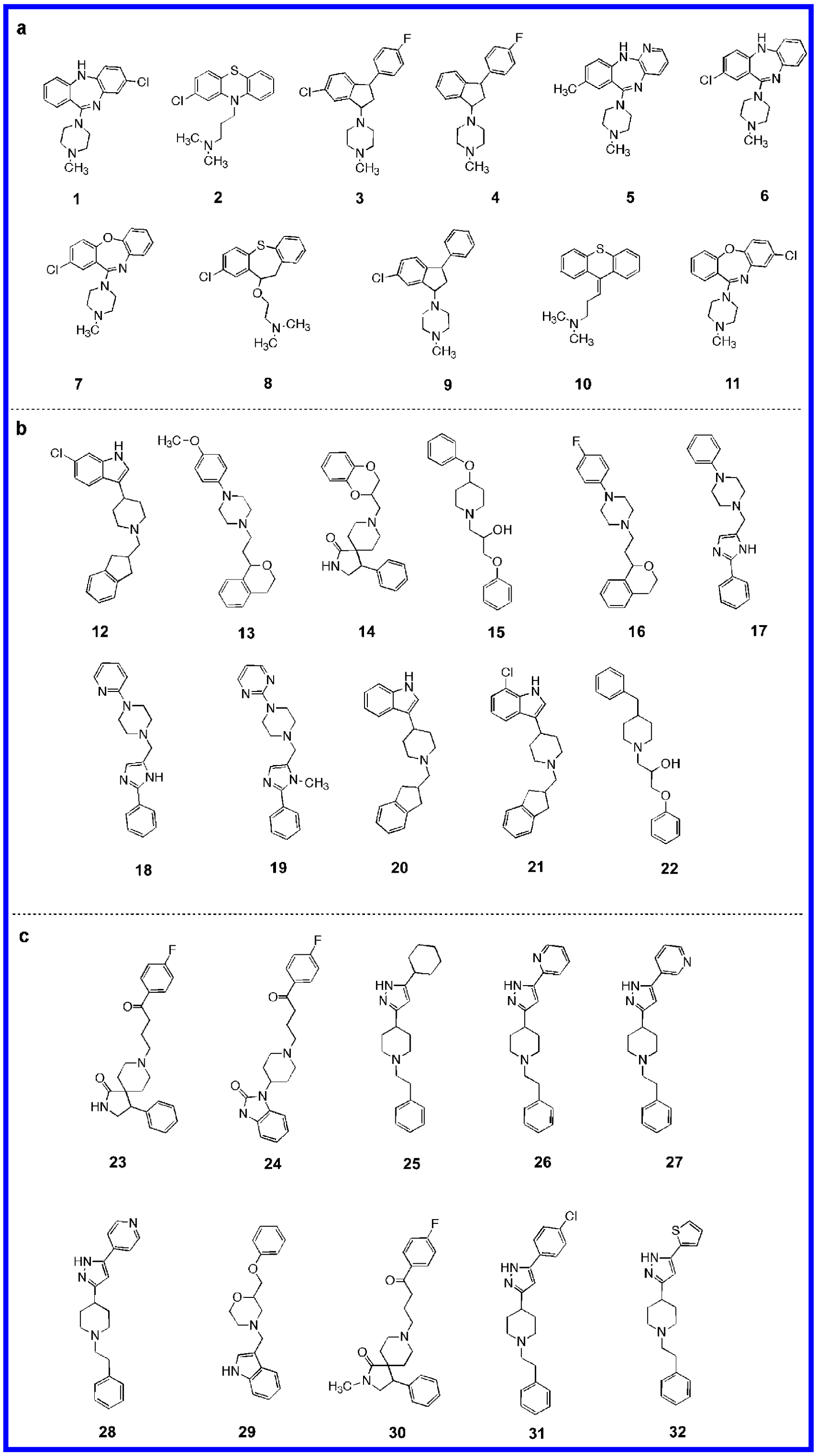

Figure 2. The structures of the ligands regarded in the training set. The ligands of the training set were selected such that approximately one-third falls into each of the three possible binding modes. (a) Compounds **1**−**11** are fitted onto the model with respect to pharmacophore elements **A**, **B**, **C**, and **D**, (b) compounds **12**−**22** are fitted on to the model with respect to pharmacophore elements **A**, **C**, **D**, and **G,** and (c) compounds **23**−**32** are fitted on to the model with respect to pharmacophore elements **B**, **C**, **D**, and **G**.

using an sp^3 carbon probe atom with a charge of +1. The CoMSIA calculations employed a standard probe atom with a radius of 1 Å and charge, hydrophobicity, and hydrogen-bond properties of +1. The standard setting (0.3) of the attenuation factor α was used. The leave-one-out cross-validation method using the SAMPLS method was employed.[32] The optimal number of components for the final 3D QSAR equation was chosen on the basis of the highest q^2 value. The minimum sigma standard deviation threshold was set to 2.0 kcal/mol and 2.0 for CoMFA and CoMSIA, respectively. The statistical results (q^2, s_{PRESS}, r^2, and S) were calculated as implemented in SYBYL. The coefficient contour maps were generated using the "stdev*coeff" field type.

The CoMSIA Procedure. The CoMFA approach employs two classical fields: Lennard-Jones potentials to describe steric interactions and Coulomb potentials to characterize electrostatic properties.[10] Both potentials display a very steep

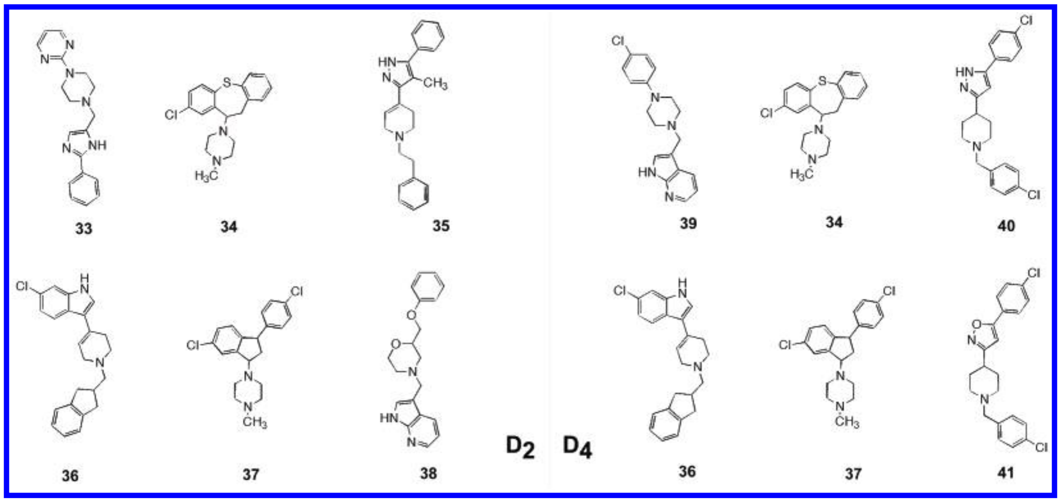

Figure 3. Ligands employed for the D_2 (left) and D_4 (right) test set.

Table 2. Experimental and Calculated Binding Constants, Given as pK_i Values, for the Dopamine D_2 Test Set Derived with CoMFA and CoMSIA

	pK_i			
		calc		
no.	exp	CoMSIA	CoMFA	ref[a]
33	5.65	5.53	6.18	22
34	8.55	8.08	7.82	13, 26
35	7.05	6.65	6.49	23
36	6.72	7.57	7.49	13, 18
37	7.71	8.38	8.26	13, 14
38	5.89	6.54	6.90	24

[a] Where two references are given, this denotes a compound tested at H. Lundbeck A/S (first reference) and listed structurally elsewhere (second reference).

Table 3. Experimental and Calculated Binding Constants, Given as pK_i Values, for the Dopamine D_4 Test Set Derived with CoMFA and CoMSIA

	pK_i			
		calc		
no.	exp.	CoMSIA	CoMFA	ref[a]
34	8.96	7.83	7.86	13, 26
36	8.12	8.83	8.83	13, 18
37	7.94	7.96	7.92	13, 14
39[b]	9.37	8.19	8.39	27
40	7.22	7.95	7.95	23
41	7.36	7.99	8.05	23

[a] Where two references are given, this denotes a compound tested at H. Lundbeck A/S (first reference) and listed structurally elsewhere (second reference). [b] It has recently been shown that **39** behaves as a partial agonist at human dopamine $D_{4.4}$ receptors expressed in CHO cells.[28]

gradient at short range. As a consequence, lattice points close to the van der Waals surface may report widely varying potential energies, depending on molecular alignment and grid spacing. For example, changing the alignment of a given molecule slightly may alter the value of a variable near the surface from being attractive to strongly repulsive. Naturally, this can profoundly affect the results. Also, since the functional forms of the Lennard-Jones and Coulomb potentials differ, and since both potentials display singularities at the atomic positions, an arbitrary energy cutoff must be employed. This can result in loss of information from one or other potential, due to the fact that the energy cutoff can be exceeded at different distances from the molecule. In addition, due to this arbitrary energy cutoff, the CoMFA contour maps are often fragmentary and noncontiguous; they only provide information about regions *outside* the defined molecular backbone. Accordingly, for a lattice point where the calculated value exceeds the predefined cutoff value, the cutoff value is recorded. As a consequence, all grid points *inside* the molecules will have the same (steric) value. Such grid points are ignored by CoMFA, because multivariate methods cannot extract information about grid points with no variance.

The CoMSIA method[11] employs similarity indices instead of the well-established physicochemical Lennard-Jones and Coulomb potentials. As with CoMFA, the similarity indices are sampled by placing a common probe at the intersections of a regularly spaced grid box. The similarity index A_F at the grid point q between a common probe and the selected compounds is calculated according to eq 1

$$A^q_{F,k}(j) = \sum_{i=1}^{n} w_{\mathrm{probe},k} w_{i,k} e^{-\alpha r_{iq}^2} \qquad (1)$$

where i equals the summation index for all atoms of molecule j; w_{ik} is the actual value of the physicochemical property k of atom i; $w_{\mathrm{probe},k}$ is the probe atom with charge +1, radius 1 Å, hydrophobicity and hydrogen property of +1; α is the attenuation factor; and r_{iq} is the mutual distance between the probe atom at grid point q and the atom i of the test molecule.

Being an extension to the CoMFA approach which has two fields, the CoMSIA method incorporates five different property fields: steric, electrostatic, hydrophobic, hydrogen-bond donor, and acceptor properties. The steric property field is expressed as the cube of the atomic radii. The electrostatic field is based on partial atomic charges. Hydrophobicities are atom-based, as parametrized by Viswanadhan and co-workers.[33] Potential locations of hydrogen-bond donor and acceptor atoms within a putative protein environment are derived from experimental values.[34,35]

It must be stressed that the CoMSIA method employs similarity fields and not the physicochemical potentials used in CoMFA (i.e. the Coulomb and Lennard-Jones potentials). The purpose of evaluating five fields is to divide the different contributions of the biological activity into specific proper-

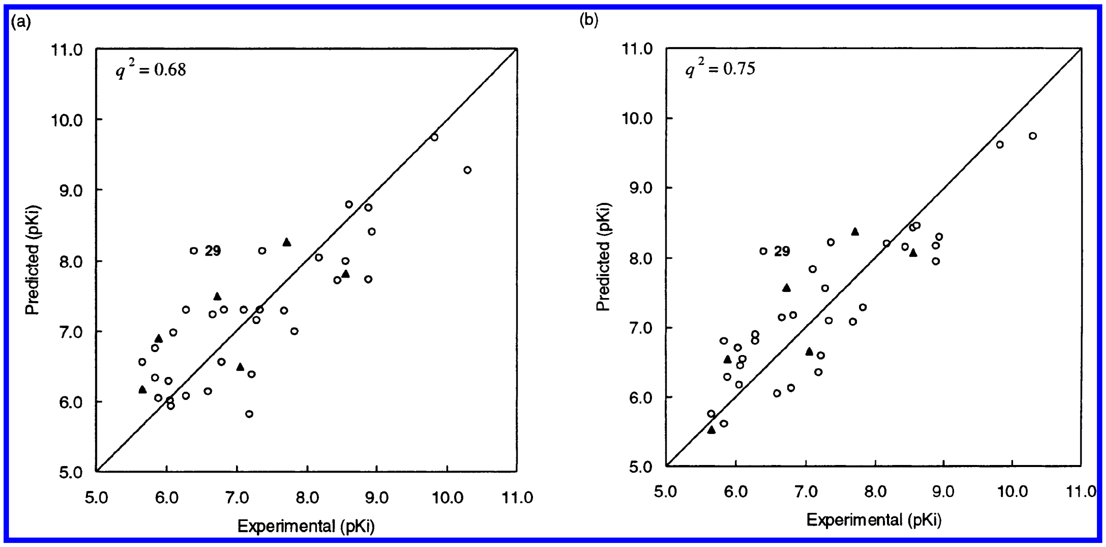

Figure 4. The experimental vs predicted D_2 biological activities obtained by the CoMFA (a) and the CoMSIA (b) analysis: ○ = training set and ▲ = test set.

Table 4. Summary of Results from the CoMSIA and CoMFA Analyses of the D_2 and D_4 Training Set

	D_2 data set		D_4 data set	
	CoMSIA	CoMFA	CoMSIA	CoMFA
		Statistical Values		
q^2	0.75	0.68	0.51	0.49
s_{PRESS}	0.65	0.74	0.48	0.49
r^2	0.92	0.88	0.77	0.74
S	0.37	0.45	0.33	0.35
components	3	3	2	2
		Fractions (%)		
steric	9.3	67.6	10.5	71.4
electrostatic	11.9	32.4	14.4	28.6
hydrophobic	24.0		18.9	
donor	14.2		18.8	
acceptor	40.7		37.5	
		Box (Step Size 1 Å)		
x	−11	9		
y	−12	9		
z	−9	15		

ties; this aids the interpretation of which factors are important for binding. For example, a favorable hydrophobic interaction is easily identified graphically—a contour map is produced specifically for this property. The similarity indices give meaningful values at all grid points since the fields for different physicochemical properties in the CoMSIA approach employ a Gaussian-type distance dependency, thereby avoiding any singularities. Thus, contrary to CoMFA, areas *within* the molecule are not excluded from the evaluation, and easily interpretable contiguous contour maps may be obtained.

In conclusion, the CoMSIA method is more intuitive and lends itself to a straightforward graphical analysis, compared with the CoMFA method. Additionally, the smooth Gaussian-type functions also ameliorate the frequently reported orientation problem. With CoMFA, the orientation of the molecular aggregate, with respect to the arbitrarily chosen grid, has significant influence on the final result.[36,37] This effect is not observed with the CoMSIA method.[38]

RESULTS AND DISCUSSION

Statistically significant CoMFA and CoMSIA models have been derived from a training set of 32 D_2 and D_4 receptor antagonists. The CoMSIA and the CoMFA methods produce equally good models expressed in terms of the q^2 values (Table 4). The better q^2 value for the D_2 models could be attributable to the greater range of experimental binding affinities among the D_2 ligands.

The predictive power of the derived models was validated using nine additional antagonists, six for each test set. The predicted vs measured pK_i values for the D_2 antagonist training and test set obtained by the two methods are shown in Tables 1−3. In both cases, the predicted values do not deviate significantly from the measured binding affinities (generally with less than one logarithmic unit). The predicted vs measured pK_i values for the D_4 and D_2 training and test sets are graphically depicted in Figures 4 and 5.

The affinity of one particular compound (**29**) from the training set was poorly predicted by the D_2 models (Figure 4). Since **29** is the only compound of its structural class, a case could be made for removing it from the training set, to increase the predictive power of the model. Therefore, the model was rederived, leaving **29** out. A slight improvement in q^2 was observed but was not significant enough to warrant its exclusion. A difference in q^2 is generally considered significant if it is greater than 0.2.[39] In addition, the use of **29** in the D_2 model as well as in the D_4 model can also be justified for comparison reasons. Two identical training sets can thus be employed.

A common validity check for 3D QSAR models is to scramble the biological data and rederive the model; the preferred model should be significantly better than those built with scrambled data, thus ruling out the possibility of chance correlations. After shuffling the data sets into several random combinations, negative q^2 values were obtained from PLS analyses without exception.

Graphical Interpreation of the Results. Not only is the CoMSIA method more robust,[38] the contour maps obtained from it are superior to the CoMFA contour maps with respect to graphical interpretation. Accordingly, the CoMSIA contour maps were used for graphical analysis.

We have previously proposed that structural features occupying region **G** (Figure 1) are of importance for determining D_2/D_4 antagonist selectivity.[9] The contour maps for *steric properties* confirm this hypothesis. The map

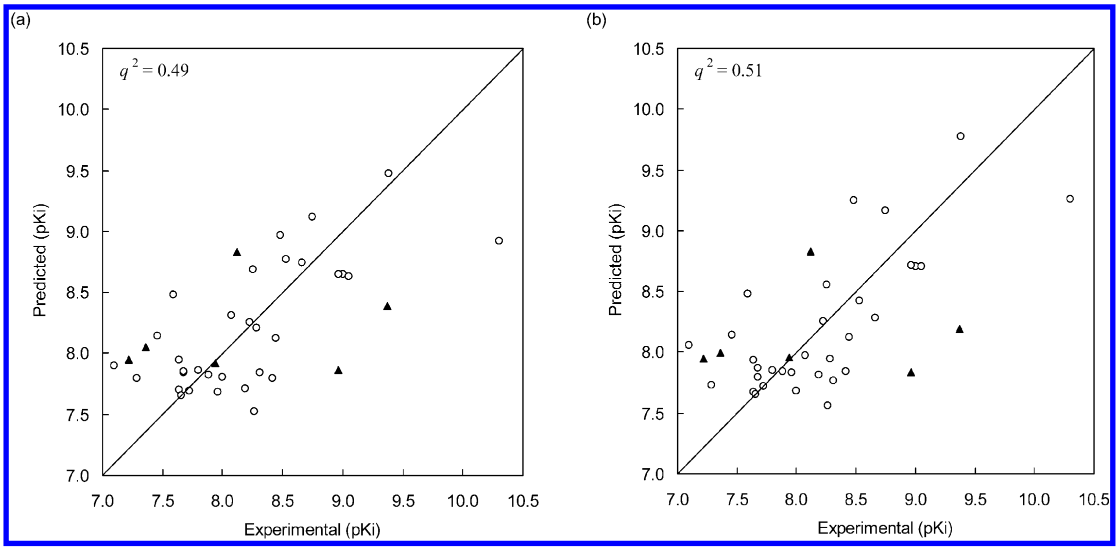

Figure 5. The experimental vs predicted D_4 biological activities obtained by the CoMFA (a) and the CoMSIA (b) analysis: ○ = training set and ▲ = test set.

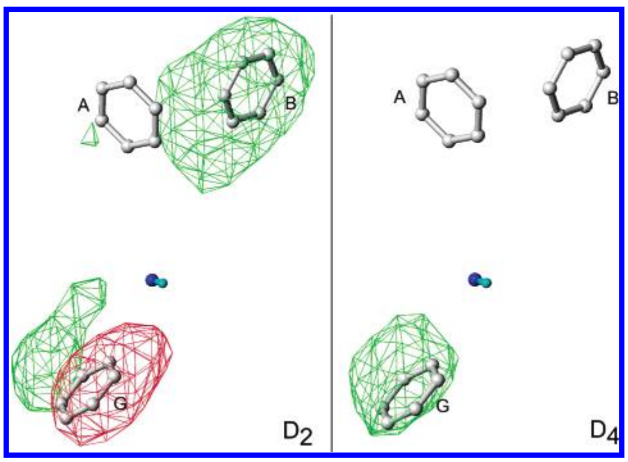

Figure 6. CoMSIA contour plots showing steric features pertaining to D_2 (left) and D_4 (right) affinities. Green contours (level 0.00068) enclose regions where steric bulk is predicted to enhance affinity. Red contours (level −0.00068) highlight regions predicted to cause unfavorable steric interactions between bulky substituents and the receptor. The introduction of bulky *N*-substituents near pharmacophore element **G** region is predicted to decrease D_2 receptor binding, whereas D_4 binding would be promoted.

obtained from the D_4 model shows a favorable region (green contour) surrounding pharmacophore element **G**, whereas the D_2 model displays a sterically unfavorable region (Figure 6). Thus, introduction of bulky *N*-substituents in this region is predicted to decrease D_2 receptor binding, whereas D_4 binding would be promoted. Furthermore, in the case of D_2 but not D_4, there is a large contour indicating steric favorability surrounding pharmacophore element **B**; the inference is that D_2 (but not D_4) affinity is highly dependent on variation of molecular steric properties within this region (Figure 6). The findings for steric properties indicate that a D_4 antagonist with selectivity over D_2 should exhibit a similiar binding mode as ligands **12**−**22** (Figure 2).

The CoMSIA contour maps for *electrostatic properties* provide insights into how to achieve D_2/D_4 selectivity. We have previously shown that electronic effects pertaining to heteroaromaticity near pharmacophore elements **B** and **G** have more influence on D_2 than on D_4 affinities.[9] The contour surrounding pharmacophore element **B** of the D_4 model shows a region (green contour) where electron-poor molecular fragments are predicted to enhance affinity. The opposite trend is noted for D_2: there is a red contour near **B** where an increase in electron density is predicted to improve affinity (Figure 7). The red contour near pharmacophore element **G** highlight a region where electron rich molecular fragments are expected to increase D_4 affinity. Again, the opposite trend is noted for D_2 (Figure 7). Furthermore, two negative (red) and one positive (green) contours exclusive to D_2 are identified. These regions should be properly taken into account when designing for lowered D_2 affinity.

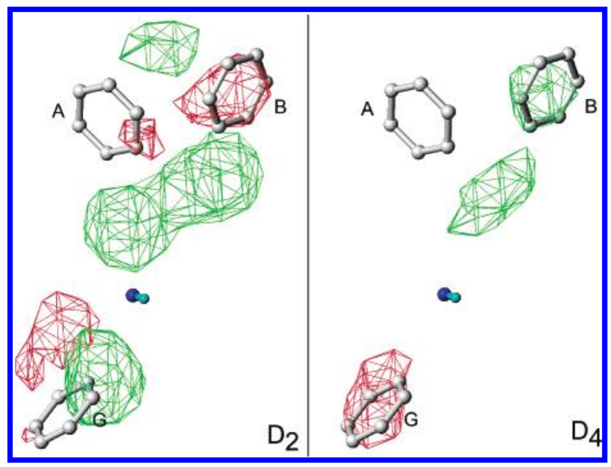

Figure 7. CoMSIA contour plots showing electrostatic properties with respect to D_2 (left) and D_4 (right) affinities. Red contours (level 0.0011) encompass regions where electron-rich fragments are predicted to improve affinity. Green contours (level −0.0011) indicate regions where fragments with reduced electron density are predicted to improve affinity. The contours near aromatic pharmacophore elements **B** and **G** show opposite trends for the D_2 and D_4 models. These regions provide suggestions as to how to obtain D_2/D_4 selectivity. Furthermore, three electrostatically important regions (two positively and one negatively charged region) exclusively identified to matter for the D_2 receptor have to be regarded correctly to design ligands discriminative for the D_2 receptor.

Figures 8 and 9 depict CoMSIA maps showing *hydrogen-bond acceptor properties*; they correspond to regions of the putative protein environment which are capable to donate hydrogen-bonds. Four regions (red contours) stand out in which the presence of a ligand hydrogen-bond acceptor decreases D_2 affinity but not D_4 affinity. Thus, these regions

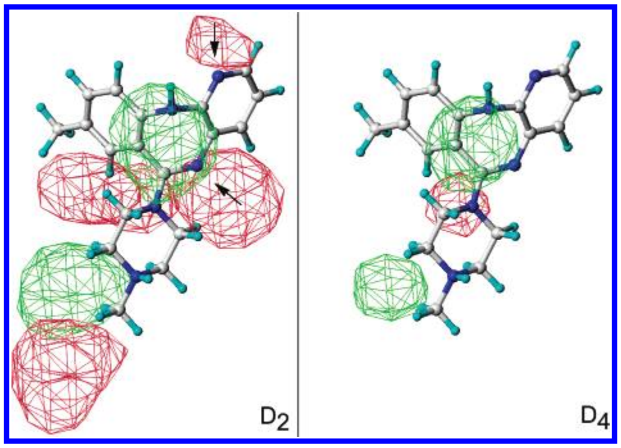

Figure 8. CoMSIA contour plots showing hydrogen-bond acceptors properties with respect to D_2 (left) and D_4 (right) affinities. Red contours (level 0.0026) enclose regions in which the presence of a ligand hydrogen-bond acceptor decreases (D_2 or D_4) receptor affinities. Green contours (level −0.0026) enclose regions in which the presence of a ligand hydrogen-bond acceptor increases (D_2 or D_4) receptor affinities. The pyridine-type and the amidine-type nitrogens of the D_4 selective pyridobenzodiazepine **5** are facing two contours, indicated with arrows, where a hydrogen-bond donor group of the putative receptor appear unfavorable in the D_2 model but not in the D_4 model. These regions seem to be important for enhancing D_2/D_4 selectivity.

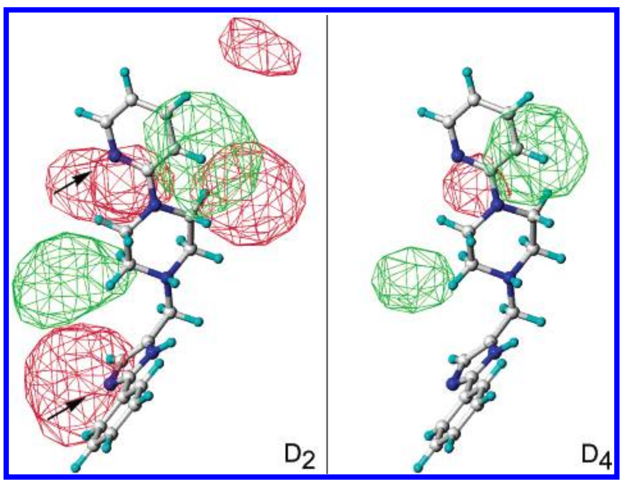

Figure 9. CoMSIA contour plots showing hydrogen-bond acceptors properties with respect to D_2 (left) and D_4 (right) affinities. Red contours (level 0.0026) enclose regions in which the presence of a ligand hydrogen-bond acceptor decreases (D_2 or D_4) receptor affinities. Green contours (level −0.0026) enclose regions in which the presence of a ligand hydrogen-bond acceptor increases (D_2 or D_4) receptor affinities. The pyridine-type and the unprotonated imidazole nitrogen of the D_4 selective compound **18** are facing two contours, indicated with arrows, where hydrogen-acceptor properties of the ligand are predicted to be unfavorable in the D_2 model but not in the D_4 model. These regions suggest how to enhance D_2/D_4 selectivity.

suggest how to enhance D_2/D_4 selectivity. The following two depictions (Figures 8 and 9) of the CoMSIA maps spell this out in detail using some representative examples. The poor D_2 binding of **5**, a clozapine (**1**) analogue, is attributable to the presence of a pyridine-type nitrogen near pharmacophore element **B**.[9] This finding is reflected in Figure 8: the pyridine nitrogen is facing a red contour where the D_2 model suggests that the presence of a ligand functional group capable to accept a hydrogen-bond is unfavorable. Likewise, the amidine nitrogen in the central ring of **5** (and by analogy in **1**, **6**−**7**, **11**) is also facing a red contour where a hydrogen-bond donor group of the putative receptor appear unfavorable in the D_2 model (Figure 8).

We have previously proposed that D_2 affinity, but not D_4 affinity, is reduced by the presence of a heterocyclic ring in the region corresponding to pharmacophore element **A**.[9] This is illustrated in Figure 9 using compound **18**, which has a pyridine-type nitrogen in this region. The pyridine nitrogen is facing a red contour where hydrogen−acceptor properties of the ligand are predicted to be unfavorable with respect to the putative D_2 receptor. Likewise, the imidazole nitrogen of **18** is facing another region where hydrogen-bond donating groups present in the D_2 receptor would be unfavorable for ligand binding.

These four red contours are not present in the D_4 model (Figures 8 and 9). When designing a D_4 selective antagonist, one could follow the example of structures **5** and **18** and include a hydrogen-bond acceptor in the regions facing the contours indicated by arrows in Figures 8 and 9.

The contour diagrams for steric, electrostatic, and hydrogen-bonding acceptor properties highlight regions likely to contribute to a discrimination between the two receptors subtypes. The contour maps of hydrogen-bonding donor and hydrophobic properties are less illuminating, since the contours for these properties are very similar among the two receptor subtypes. They do not assist in the discussion on D_2/D_4 selectivity, and accordingly they are not shown. Furthermore, as obvious from Table 4 the hydrogen-bond acceptor property contributes significantly more to the derived CoMSIA models.

CONCLUSIONS

A 3D QSAR study has been performed in order to obtain a more detailed insight into the structure−activity relationships of D_4 and D_2 receptor antagonists, beyond the usual features apparent from pharmacophore models. Statistically significant models have been derived with two methods, CoMFA and CoMSIA, based on a set of 32 structurally diverse D_2 and D_4 receptor antagonists. The CoMSIA and the CoMFA methods produce equally good models expressed in terms of the q^2 values. The predictive power of the derived models were demonstrated to be reliable.

One of the main goals was to investigate which structural features give rise to selectivity for D_4 over D_2. Graphical interpretation of the results, provided by the CoMSIA method, brings to light important structural features that could be responsible for either low- or high-affinity D_2 or D_4 antagonism. The contours for steric, electrostatic, and hydrogen-bond acceptor properties highlight regions discriminating between the two receptor subtypes. The contour diagrams for steric properties reveal that bulky *N*-substituted ligands are likely to decrease D_2 binding, whereas D_4 binding would be enhanced. The D_2 and D_4 contour diagrams for electrostatic properties show opposite trends near the two aromatic pharmacophore elements **B** and **G**. Furthermore, three electrostatically important regions (two negative regions and one positive region) exclusively identified to matter for the D_2 receptor have to be regarded correctly to design ligands discriminative for the D_2 receptor. Likewise, the incorporation of hydrogen-bond acceptors into ligands could result in a lower D_2 affinity.

ACKNOWLEDGMENT

J.B. thanks Dr. Jeremy Greenwood for linguistic criticism. This work was financially supported by the NeuroScience PharmaBiotec Centre and the Lundbeck Foundation which is gratefully acknowledged.

Supporting Information Available: The atomic coordinates of all molecules of the data set. This material is available free of charge via the Internet at http://pubs.acs.org.

REFERENCES AND NOTES

(1) a. Seeman, P. Dopamine receptors and the hypothesis of schizophrenia. *Synapse* **1987**, *1*, 133−152. b. Carlsson, A. The current status of the dopamine hypothesis of schizophrenia. *Int. Clin. Psychopharmacol.* **1988**, 1, 179−186. c. Grace, A. A. Phasic versus tonic dopamine release and the modulation of dopamine system responsivity: a hypothesis for the ethiology of schizophrenia. *Neuroscience* **1991**, *41*, 1−24.
(2) Van Tol, H. H. M.; Bunzow, J. R.; Guan, H.-C.; Sunahara, R. K.; Seeman, P.; Niznik, H. B.; Civelli, O. Cloning of the gene for human dopamine D_4 receptor with high affinity for the antipsychotic clozapine. *Nature* **1991**, *350*, 610−614.
(3) Hadley, M. S. D_4 receptors and their antagonists. *Medicinal Res. Rev.* **1996**, *16*, 507−526.
(4) Kulagowski, J. J.; Patel, S. Dopamine D4 Receptor Antagonists. *Curr. Pharm. Design* **1997**, *3*, 355−366.
(5) Steiner, G.; Bach, A.; Bialojan, S.; Greger, G.; Hege, H.-G.; Höger, T.; Jochims, K.; Munschauer, R.; Neumann, B.; Teshendorf, H.-J.; Traut, M.; Unger, L.; Gross, G. $D_4/5HT_{2A}$ receptor antagonists: LU-111995 and other potential new antipsychotics in development. *Drugs Future* **1998**, *23*, 191−204.
(6) Casey, D. E. Neuroleptic drug-induced extrapyramidal syndromes and tardive dyskinesia. *Schizophrenia Res.* **1991**, *4*, 109−120.
(7) Matsumoto, M.; Hidaka, K.; Tada, S.; Tasaki, Y.; Yamaguchi, T. Full-length cDNA and distribution of the human D_4 receptor. *Mol. Brain Res.* **1995**, *29*, 157−162.
(8) Amsler, H. A.; Teerenhovi, L.; Bartha, E.; Harjula, K.; Vuopio, P. Agranulocytosis in patients treated with clozapine: a study of the Finnish epidemic. *Acta Psychiatr. Scand.* **1977**, *56*, 241−248.
(9) Boström, J.; Gundertofte, K.; Liljefors, T. A pharmacophore model for dopamine D4 receptor antagonists. *J. Comput.-Aid. Mol. Des.* **2000**, *14*, 769−786.
(10) Cramer, R. D., III; Patterson, D. E.; Bunce, J. D. Comparative molecular field analysis (CoMFA). 1. Effect of shape on binding of steroids to carrier proteins. *J. Am. Chem. Soc.* **1988**, *110*, 5959−5967.
(11) Klebe, G.; Abraham, U.; Mietzner, T. Molecular similarity in a comparative analysis (CoMSIA) of drug molecules to correlate and predict their biological activity. *J. Med. Chem.* **1994**, *37*, 4130−4146.
(12) Lanig, H.; Gmeiner, P.; Utz, W. Comparative Molecular Field Analysis of Dopameine D4 Receptor Antagonists Including 3-[4-(4-Chlorophenyl)piperazin-1-ylmethyl]pyrazolo[1,5-α]pyridine (FAUC 113), 3-[4-(4- Chlorophenyl)piperazin-1-ylmethyl]-1*H*-pyrrolo-[2,3-*b*]pyridine (L-745,870), and Clozapine. *J. Med. Chem.* **2001**, *44*, 1151−1157.
(13) Lundbeck, H. A/S unpublished data.
(14) Palm, J.; Bøgesø, K. P.; Liljefors, T. A structure−activity study of four dopamine D-1 and D-2 receptor antagonists, representing the phenylindan, -indene and -indole structural classes of compounds. *J. Med. Chem.* **1993**, *36*, 2878−2885.
(15) Liegeois, J.-F.; Bruhwyler, J.; Damas, J.; Rogister, F.; Masereel, B.; Geczy, J.; Delarge, J. Modulation of the clozapine structure increases its selectivity for the dopamine D4 receptor. *Eur. J. Pharmacol.* **1995**, *273*, R1−R3.
(16) Janssen, P. A. J.; Awouters, F. H. L. Is it possible to predict the clinical effects of neuroleptics from animal data? Part V: from haloperidol and pipamperone to risperidone. *Arzneim. Forsch.* **1994**, *44*, 269−277.
(17) Froimowitz, M.; Cody, V. Biological active conformers of phenothiazines and thioxanthenes. Further evidence for a ligand model of dopamine D2 receptor antagonists. *J. Med. Chem.* **1993**, *36*, 2219−2227.
(18) Perregaard, J.; Bang-Andersen, B.; Pedersen, H.; Mikkelsen, I.; Dancer, R. WO-9828293, 1998.
(19) TenBrink, R. E.; Berg, C. L.; Duncan, J. N.; Harris, D. W.; Huff, R. M.; Lahti, R. A.; Lawson, C. F.; Lutzke, B. S.; Martin, I. J.; Rees, S. A.; Schlachter, S. K.; Sih, J. C.; Smith, M. W. (S)-(−)-4-[4-[2-(isochroman-1-yl)ethyl]-piperazin-1-yl]benzene sulfonamide, a selective dopamine D4 antagonist. *J. Med. Chem.* **1996**, *39*, 2435−2437.
(20) Nikam, S. S.; Martin, A. R.; Nelson, D. L. Serotonergic properties of spiroxatrine enantiomers. *J. Med. Chem.* **1988**, *31*, 1965−1968.
(21) Wright, J. L.; Gregory, T. F.; Heffner, T. G.; MacKenzie, R. G.; Pugsley, T. A.; Vander Meulen, S.; Wise, L. D. Discovery of selective dopamine D4 receptor antagonists: 1-aryloxy-3-(4-aryloxypiperidinyl)-2-propanols. *Bioorg. Med. Chem. Lett.* **1997**, *7*, 1377−1380.
(22) Thurkauf, A.; Yuan, J.; Chen, X.; Shu, X.; Wasley, J. W. F.; Hutchison, A.; Woodruff, K. H.; Meade, R.; Hoffman, D. C.; Donavan, H.; Jones-Hertzog, D. K. 2-Phenyl-4(5)-[[4-(pyrimidin-2-yl)piperazine-yl]methyl]-imidazole. A highly selective antagonist at cloned human D4 receptors. *J. Med. Chem.* **1997**, *40*, 1−3.
(23) Rowley, M.; Collins, I.; Broughton, H. B.; Davey, W. B.; Baker, R.; Emms, F.; Marwood, R.; Patel, S.; Patel, S.; Ragan, C. I.; Freedman, S. B.; Ball, R.; Leeson, P. D. 4-Heterocyclylpiperidines as selective high-affinity ligands at the human dopamine D4 receptor. *J. Med. Chem.* **1997**, *40*, 2374−2385.
(24) Showell, G. A.; Emms, F.; Marwood, R.; O'Connor, D.; Patel, S.; Leeson, P. D. Binding of 2,4-disubstituted morpholines at human D4 dopamine receptors. *Bioorg. Med. Chem. Lett*. **1998**, *6*, 1−8.
(25) a. Seeman, P.; Niznik, H. B. Dopamine D1 receptor pharmacology. *ISI Atlas of Sci. Pharmacol.* **1988**, *2*, 161−170. b. Seeman, P.; Van Tol, H. H. M. 1993, unpublished.
(26) Liljefors, T.; Bøgesø, K. P. Conformational analysis and structural comparison of (1R,3S)-(+)- and (1S,3R)-(tefludazine, (S)-(+)- and (R)-(−)-octoclothepin, and (+)-dexclamol in relation to dopamine receptor antagonism and amine-uptake inhibition. *J. Med. Chem.* **1988**, *31*, 306−312.
(27) Kulagowski, J. J.; Broughton, H. B.; Curtis, N. R.; Mawer, I. M.; Ridgill, M. P.; Baker, R.; Emms, F.; Freedman, S. B.; Marwood, R.; Patel, S.; Ragan, C. I.; Leeson, P. D. 3-[[4-(4-Chlorophenyl)piperazin-1-yl]-methyl]-1H-pyrrolo[2,3-b]pyridine: an antagonist with high affinity and selectivity for the human dopamine D4 receptor. *J. Med. Chem.* **1996**, *39*, 1941−1942.
(28) Gazi, L.; Bobirnac, I.; Danzeisen, M.; Schüpbach, E.; Bruinvels, A. T.; Langenegger, D.; Sommer, B.; Hoyer, D.; Triclebank, M.; Schoeffter, P. Receptor density as a factor governing the efficacy of the dopamine D4 receptor ligands, L-745,870 and U-101958 at human recombinant D4.4 receptors expressed in CHO cells. *Br. J. Pharmacol*. **1999**, 128, 613−620.
(29) SYBYL molecular modeling software; TRIPOS Inc., 1699 South Hanley Road, Suite 303, St. Louis, MO 63144.
(30) MOPAC: a general molecular orbital package; QCPE #445, Stewart, J. J. P., Frank, J., Seiler Bokstav Research Laboratory, United Air Force Academy, CO 80840.
(31) Stewart, J. J. P. MOPAC: a semiempirical molecular orbital program. *J. Comput.-Aided. Mol. Des.* **1990**, *4*, 1−105.
(32) Bush, L.; Nachbar, R. B., Jr. Sample-distance partial least squares: PLS optimized for many variables, with application to CoMFA. *J. Comput.-Aided. Mol. Des.* **1993**, *7*, 587−619.
(33) Viswanadhan, V. N.; Ghose, A. K.; Revankar, G. R.; Robins, R. K. Atomic physicochemical parameters for three-dimensional structure directed quantitative structure- activity relationships. 4. Additional parameters for hydrophobic and dispersive interactions and their application for an automated superimposition of certain naturally occurring nucleoside antibiotics. *J. Chem. Inf. Comput. Sci.* **1989**, *29*, 163−172.
(34) Klebe, G. The use of composite crystal-field environments in molecular recognition and the de novo design of protein ligands *J. Mol. Biol.* **1994**, *237*, 212−235.
(35) Klebe, G.; Mietzner, T.; Weber, F. Methodological developments and strategies for a fast flexible superposition of drug-size molecules. *J. Comput.-Aided Mol. Des.* **1999**, *13*, 35−49.
(36) Cho, S. J.; Tropsha, A. Cross-validated R2-guided region selection for comparative molecular field analysis: a simple method to achieve consistent results. *J. Med. Chem.* **1995**, *38*, 1060−1066.
(37) Kim, K. H.; Brusniak, M. K.; Pearlman, R. S. UniSurCoMFA: for stable and consistent 3D QSAR. In *Rational Molecular Design in Drug Research*; Liljefors, T., Jørgensen, F. S., Krogsgaard-Larsen, P., Eds.; Munksgaard: Copenhagen, 1998; pp 67−83.
(38) Böhm, M.; Stürzebecher, J.; Klebe, G. 3D QSAR Analyses using CoMFA and CoMSIA to elucidate selectivity differences of inhibitors binding to trypsin, thrombin and factor Xa. *J. Med. Chem.* **1999**, *42*, 458−477.
(39) Cramer, R. D.; DePriest, S. A.; Patterson, D. E.; Hecht, P. The developing practice of comparative molecular field analysis. In *3D QSAR in Drug Design: Theory, Methods and Applications*; Kubinyi, H., Ed.; ESCOM: Leiden, 1993; pp 443−485.

CI034004+